═══REVIEW COMMONS MANUSCRIPT═══

IMPORTANT:

- Manuscripts submitted to Review Commons are peer reviewed in a journal-agnostic way.
- Upon transfer of the peer reviewed preprint to a journal, the referee reports will be available in full to the handling editor.
- The identity of the referees will NOT be communicated to the authors unless the reviewers choose to sign their report.
- The identity of the referee will be confidentially disclosed to any affiliate journals to which the manuscript is transferred.

GUIDELINES:

- For reviewers: https://www.reviewcommons.org/reviewers
- For authors: https://www.reviewcommons.org/authors

CONTACT:

The Review Commons office can be contacted directly at: office@reviewcommons.org

Desert Hedgehog mediates stem Leydig cell differentiation through Ptch2/Gli1/Sf1 signaling axis

Changle Zhao, Yongxun Chen, Lei Liu, Xiang Liu, Hesheng Xiao, Feilong Wang, Qin Huang, Xiangyan Dai, Wenjing Tao, Deshou Wang*, Jing Wei*

Author affiliations: Integrative Science Center of Germplasm Creation in Western China (CHONGQING) Science City, Key Laboratory of Freshwater Fish Reproduction and Development (Ministry of Education), Laboratory of Aquatic Science of Chongqing, School of Life Sciences, Southwest University, Chongqing 400715, China

Prof. Deshou Wang, E-mail address: wdeshou@swu.edu.cn. Tel.: (86) 023 68252702; Fax: (86) 023 68253005.

Prof. Jing Wei, E-mail address: lalsos@swu.edu.cn. Tel.: (86) 023 68252365; Fax: (86) 023 68253005.

Abstract

Desert Hedgehog (Dhh) mutations cause male infertility, testicular dysgenesis and Leydig cell dysfunction. However, the mechanisms by which Dhh regulates Leydig lineage commitment through receptor selectivity, transcriptional effector specificity, and steroidogenic coupling remain elusive. In this study, we identified a Dhh-Ptch2-Gli1-Sf1 signaling axis that is essential for the differentiation of stem Leydig cells (SLCs) by using CRISPR/Cas9-generated *dhh*/*ptch2* mutants of Nile tilapia (*Oreochromis niloticus*) and SLC transplantation. The loss of Dhh recapitulated mammalian phenotypes, characterized by testicular hypoplasia and androgen insufficiency. Rescue experiments with 11-ketotesterone and a Dhh agonist, in conjunction with SLC transplantation, demonstrated that Dhh regulates the differentiation of SLCs rather than their survival. *In vitro* knockout experiments of *ptch1* and *ptch2* in SLCs indicated that Patched2 (Ptch2), rather than Ptch1, serves as the receptor for Dhh in SLCs. Furthermore, *in vivo* genetic rescue experiments indicated that while the *ptch2* mutation did not affect testicular development, the Ptch2 mutation fully rescued the developmental disorders of the testes caused by the *dhh* mutation, thereby further corroborating Ptch2 as the receptor for Dhh in SLCs. Additionally, the Glioma-associated oncogene homolog 1 (Gli1, but not Gli2 or Gli3) functions as the transcriptional effector that drives the expression of steroidogenic factor 1 (*sf1*). Transcriptomic and functional analyses further established that Dhh signaling directly couples Sf1 to SLC differentiation. This study provides mechanistic insights into Dhh-related Leydig cell dysfunction and presents novel targets for regenerative therapies.

Keywords: Stem Leydig cells, Differentiation, Dhh, Ptch2, Sf1

Highlights

- Dhh regulates the differentiation of SLCs rather than their survival
- Ptch2, rather than Ptch1, is the specific receptor for Dhh in SLCs
- Gli1, not Gli2 or Gli3, is the principal transcriptional activator of Dhh in SLCs
- Sf1 is a direct transcriptional target of Gli1 in SLCs differentiation

INTRODUCTION

Testicular development requires precise coordination of somatic cell interactions, with Leydig cells producing approximately 95% of circulating androgens to sustain spermatogenesis and male fertility [1, 2]. Leydig cells originate from stem Leydig cells (SLCs), which differentiate into steroidogenic adult Leydig cells (ALCs) under paracrine regulation [3, 4]. Steroidogenic Factor 1 (SF1), an orphan nuclear receptor transcription factor, serves as a master regulator of this process by activating steroidogenic enzymes (e.g., cytochrome P450, family 11, subfamily C, polypeptide 1 [Cyp11c1], 3β-hydroxysteroid dehydrogenase [3β-HSD]) to drive ALC maturation [5]. In mice, mutations of *Sf1* exhibit arrested testicular development and abolished steroidogenesis [6, 7], while human *SF1* mutations are associated with 46,XY disorders of sexual development (DSD), such as Swyer syndrome [8]. Similarly, in Nile tilapia (*Oreochromis niloticus*), our previous work reveals that *sf1* mutation disrupts testicular morphogenesis and downregulates the expression of key steroidogenic enzymes such as *cyp11c1* and cytochrome P450, family 19, subfamily A, polypeptide 1a (*cyp19a1a*) [9]. Despite its central role, the upstream signaling mechanisms controlling SF1-mediated Leydig lineage commitment remain elusive.

Hedgehog (Hh) signaling pathway is an evolutionarily conserved developmental regulator [10]. Canonical Hh signaling involves the binding of ligands to Patched (Ptch) receptors, which relieves the suppression on Smoothened (Smo) and ultimately activates Glioma-associated oncogene homolog (Gli) transcription factors to regulate target genes [11-13]. In vertebrates, there are three Hh ligands (i.e. Sonic Hh, Indian Hh and Desert Hh [Dhh]), two Ptch receptors (Ptch1 and Ptch2) and three Gli homologs (Gli1-3) [14-16]. A large number of studies have well demonstrated that Dhh signaling pathway is critical in gonadal development [13, 17]. Dhh, secreted by Sertoli cells, is critical for Leydig cell commitment in mammals [18, 19]. In mice, mutations of *Dhh* lead to Leydig cell dysfunction, testosterone insufficiency, and infertility [20], while human *DHH* mutations are associated with 46,XY DSD [21]. Strikingly, these phenotypes mirror those caused by *Sf1* deficiencies, suggesting a potential regulatory nexus between Dhh and SF1 signaling. However, the molecular mechanisms remain

unresolved.

Studies demonstrate functional divergence between Ptch1 and Ptch2. For instance, *Ptch1* knockout causes embryonic lethality due to constitutive Hh activation, whereas *Ptch2* deficiency yields no overt defects [22, 23]. During testicular development, Ptch1 displays high early expression critical for gonadal primordium formation, while Ptch2 shows testis-enriched dynamic regulation [24, 25]. However, the distinct roles of Ptch1 and Ptch2 in Leydig lineage commitment remain unknown to date. Among Gli transcription factors, Gli1 acts as a primary activator, while Gli2 and Gli3 exhibit dual regulatory functions [26, 27]. In murine testes, co-expression of Gli1 and Gli2 in Leydig cells illustrates functional redundancy—single knockouts show normal development, but combined pharmacological inhibition (GANT61) abolishes Leydig cells and spermatogenesis [28]. Nevertheless, the mechanisms underlying Gli-mediated Leydig lineage still require further investigation.

Nile tilapia (*Oreochromis niloticus*) serves as an excellent model for studying gene function and endocrine mechanisms due to its XX/XY sex-determining system [29], short spawning cycle (approximately 14 days), year-round artificial reproduction capabilities in the laboratory [30], well-developed sex-linked genetic markers [31], and moderate size suitable for blood and hormone assays. Importantly, we have developed a clonal stem Leydig cell line (TSL) from the testis of a 3-month-old Nile tilapia. This cell line expresses stem Leydig cell markers, including platelet-derived growth factor receptor α (*pdgfrα*), *nestin*, and chicken ovalbumin upstream promoter transcription factor II (*coup-flla*) [32]. Upon induced differentiation, TSL expresses steroidogenic genes such as steroidogenic acute regulatory protein 1 (*star1*), *star2*, *cyp11c1*, and cytochrome P450, family 17, subfamily A, polypeptide 2 (*cyp17a2*), leading to the production of 11-ketotestosterone (11-KT) [9, 32]. In this study, by combining $dhh^{-/-}$ XY fish with TSL transplantation technology, we unveil a Dhh-Ptch2-Gli1-Sf1 axis that is essential for Leydig lineage differentiation. Our findings not only clarify mechanistic ambiguities in Dhh-mediated Leydig lineage commitment but also establish Nile tilapia as a unique comparative model for dissecting stem cell niche interactions, with implications for understanding male infertility and regenerative therapies.

RESULTS

Mutation of *dhh* disrupts testicular organization and androgen synthesis

Nile tilapia Dhh open reading frame (ORF; 1377 bp) was cloned and validated (GenBank ID: 100707022). The encoded 458-amino acid protein shares over 56% identity with vertebrate homologs (Fig. S1A) and clusters phylogenetically with mammalian DHH orthologs (Fig. S1B). Transcriptomic analyses conducted on various tissues and testes across different developmental stages revealed that *dhh* expression peaked in the testes, particularly at 90 days after hatching (dah) (Fig. S1C, D).

CRISPR/Cas9 targeting of *dhh* exon 1 from Nile tilapia generated homozygous mutants ($dhh^{-/-}$) harboring a 13-bp frameshift deletion (Fig. S2A–D), resulting in premature termination and loss of the conserved Hedge domain (Fig. S2E). *dhh* mRNA levels in $dhh^{-/-}$ fish were significantly reduced compared to WT (Fig. S2F). At 90 dah, $dhh^{-/-}$ testes exhibited marked atrophy (Fig. 1A, B) and disorganized histology, with sparse spermatogonia, rare spermatids, and collapsed interstitial architecture (Fig. 1C–D', K). Immunofluorescence (IF) confirmed significantly reduced germ cell (Vasa+), meiotic (Sycp3+), and Leydig cell (Cyp11c1+) populations (Fig. 1E-J', L-N). Serum 11-KT levels in $dhh^{-/-}$ fish were significantly lower than WT (Fig. 1O), indicating impaired androgen synthesis.

11-KT partially rescued the number and differentiation of germ cells, but not Leydig cells

Considering the critical role of 11-KT in the testis development and spermatogenesis in teleosts [33], we tested whether 11-KT supplementation could reverse testicular defects in $dhh^{-/-}$ mutants. Exogenous 11-KT (dose - simulation of physiological levels) partially restored germ cell dynamics: H&E staining and IF analyses showed that, compared with the untreated mutants, the $dhh^{-/-}$+11-KT testes showed significantly increased germ cells (Vasa+) and spermatocytes (Sycp3+), as well as a more organized testicular structure (Fig. 2A-F', J-L', N, P), which was also supported by GSI analysis (Fig. 2M). However, Cyp11c1 positive Leydig cells remained unrecovered in $dhh^{-/-}$+11-KT testes (Fig. 2G-I', O), confirming androgen-

independent Leydig cell impairment.

Mutation of *dhh* blocks SLCs differentiation without impairing survival

To dissect Leydig cell lineage impairment in *dhh*$^{-/-}$ testes, we transplanted the TSL into WT and *dhh*$^{-/-}$ testes (Fig. 3A). In WT recipients, TSL cells colonized the interstitium and differentiated into Cyp11c1 positive steroidogenic cells (Fig. 3B1–B3). In *dhh*$^{-/-}$ testes, TSL engrafted equivalently but failed to express Cyp11c1 (Fig. 3C1–C3), indicating a differentiation-specific block. Rescue experiments showed that the TSL overexpressing Dhh (TSL-*On*Dhh) or treated with the Hedgehog agonist SAG (TSL+SAG) restored Cyp11c1 expression in *dhh*$^{-/-}$ testes (Fig. 3D1–E3, F) and a significant increase in endogenous 11-KT levels (Fig. 3G). These results suggest that SLC differentiation is inhibited in *dhh*$^{-/-}$ XY tilapia testes. Furthermore, TSL survival was unaffected in *dhh*$^{-/-}$ testes (Fig. 3C3), and continuous SAG treatment via intraperitoneal injection (30–90 dah) rescued endogenous Cyp11c1 positive Leydig cells (Fig. 3H, I), confirming that *dhh* regulates SLCs differentiation, not their survival.

To assess whether *dhh* mutation affects androgen-producing cells outside Leydig cells, 11-KT levels were analyzed during early testicular development before SLCs differentiation. IF analyses revealed that no Cyp11c1 positive cells were present in the testes of XY WT fish at 5, 10, and 20 dah, indicating that SLCs had not yet differentiated at these stages (Fig. S3A-C). Tissue fluid 11-KT levels showed no significant differences between WT and *dhh*$^{-/-}$ XY fish at 5, 10, and 20 dah (Fig. S3D). These results indicate that the impairment of androgen production in *dhh* mutations is specific to SLCs.

Ptch2 is the specific receptor for Dhh in SLCs

RT-PCR results showed that both *ptch1* and *ptch2* were expressed in TSL (Fig. S4). Fluorescence *in situ* hybridization (FISH) and IF revealed co-expression of *ptch1* and *ptch2* in Cyp11c1 positive Leydig cells (Fig. 4A, B). To identify specific receptor mediating Dhh signaling, we established *ptch1*$^{-/-}$ and *ptch2*$^{-/-}$ TSL cell lines (Figs. S5A, B) and evaluated pathway activity using an 8×GLI luciferase reporter system (Fig. 4C). In WT TSL cells, the 8×GLI reporter demonstrated substantial luciferase activity that was markedly enhanced by *On*Dhh overexpression (Fig. 4D),

confirming Dhh responsiveness in this system. Intriguingly, while *ptch1*$^{-/-}$ cells maintained Dhh-induced luciferase activation comparable to WT controls, *ptch2*$^{-/-}$ cells completely lost this responsiveness (Fig. 4E). This differential receptor requirement demonstrates that Ptch2, but not Ptch1, is specifically required for transducing Dhh signals in TSL cells.

To investigate the function of Ptch2 *in vivo*, we generated *ptch2*$^{-/-}$ and *dhh*$^{-/-}$;*ptch2*$^{-/-}$ mutant Nile tilapias (Figs. S6A-E). Compared to WT fish at 90 dah, *ptch2*$^{-/-}$ testes exhibited no significant differences in testicular histology (Fig. 4F–F', S7A–A'), GSI (Fig. 4N), germ cell (Vasa+, Sycp3+) and Leydig cell (Cyp11c1+) populations (Fig. 4H-L', O-Q, S7 B-D'), and serum 11-KT levels (Fig. 4R). Strikingly, dual knockout of *dhh*$^{-/-}$;*ptch2*$^{-/-}$ rescued the *dhh*$^{-/-}$ phenotype and exhibited normal testicular development, including testicular histology (Fig. 1D–D', 4G–G'), Leydig cell differentiation (Fig. 1H-H', 4K-K'), and serum 11-KT levels (Fig. 4R). This genetic epistasis demonstrates that Ptch2 acts as the obligate receptor for Dhh signaling during testis development.

Gli1 is the principal transcriptional effector of Dhh signaling in SLCs

In the Hh pathway, Gli transcription factors (Gli1/2/3) mediate diverse developmental processes (26). RT-PCR results showed that *gli1*, *gli2*, and *gli3* were all expressed in TSL (Fig. S4). FISH and IF revealed co-expression of *gli1*, *gli2*, and *gli3* in Cyp11c1 positive Leydig cells (Fig. 5A–C). To identify Dhh-specific effectors, we generated *gli1*$^{-/-}$, *gli2*$^{-/-}$, and *gli3*$^{-/-}$ TSL lines (Fig. S5C–E) and assessed pathway activity using the 8×GLI luciferase reporter. While TSL-*gli2*$^{-/-}$ and TSL-*gli3*$^{-/-}$ cell lines maintained Dhh-induced luciferase activation comparable to WT controls, the TSL-*gli1*$^{-/-}$ cell line completely lost this responsiveness (Fig. 5D), suggesting exclusive reliance on Gli1 for Dhh signal transduction.

Sf1 is a direct transcriptional target of Gli1 in SLCs differentiation

To identify Gli1-dependent targets in SLCs, we compared transcriptomes of TSL-WT, Dhh-overexpressing (TSL-*On*Dhh), Gli1-overexpressing (TSL-*On*Gli1), and SAG-treated (TSL+ SAG) TSL cells. RNA-seq revealed 33 upregulated and 111 downregulated genes across all three conditions (Fig. 5E, S8A). Furthermore, cluster analysis (Fig. S8B), qRT-PCR validation (Fig. S8C), and promoter analysis were

conducted on these significantly upregulated genes. Among these, *sf1* emerged as a top candidate, with its promoter (−5015 bp) harboring two conserved Gli1-binding motifs (B1/B2; Fig. 5F). Dual-luciferase assays confirmed Gli1 significantly upregulates the transcriptional activity of *sf1* (Fig. 5G).

Functional validation using *sf1*$^{-/-}$ and Sf1-overexpressing (*On*Sf1) TSL lines (Fig. S7) demonstrated that Sf1 is essential for SLCs differentiation: TSL-*sf1*$^{-/-}$ failed to express Cyp11c1 even in WT testes, while TSL-*On*Sf1 expressed Cyp11c1 in *dhh*$^{-/-}$ testes (Fig. 5H–J). These data position Sf1 as the critical mediator of SLCs differentiation.

DISCUSSION

This study delineates a critical Dhh-Ptch2-Gli1-Sf1 signaling axis essential for SLCs differentiation in Nile tilapia. By combining *dhh*$^{-/-}$ XY models with TSL cell transplantation, we demonstrate that Dhh signaling directly regulates Leydig lineage differentiation through Ptch2, independent of Ptch1, with Gli1 acting as the key transcriptional effector that activates *sf1* expression. Furthermore, Sf1 serves as the critical downstream target that bridges Dhh signaling to steroidogenic maturation. These findings resolve longstanding ambiguities in Dhh-mediated SLCs differentiation and provide evolutionary insights into vertebrate reproductive biology.

The central role of Dhh in testicular development aligns with its conserved function across vertebrates. In mice, mutation of *Dhh* leads to testosterone insufficiency, and infertility [20]. Similarly, human *DHH* mutations are associated with 46,XY DSD [21]. However, the specific mechanisms of its action in the testis remain unclear. Here, the *dhh*$^{-/-}$ tilapia phenocopied these defects, exhibiting arrested testis development, and impaired Leydig cells and 11-KT (Fig. 1). Crucially, TSL transplantation revealed that Dhh acts not on SLC survival but on differentiation: WT TSLs failed to express Cyp11c1 in *dhh*$^{-/-}$ testes unless activated by Dhh or the Hh agonist SAG, and SAG significantly promoted the number of Cyp11c1 positive cells in *dhh*$^{-/-}$ testes (Fig. 3). This highlights Dhh as a niche signal driving SLC differentiation, with androgen deficiency being secondary to lineage arrest (Fig. 2). Our model thus uncovers a causal chain from Dhh loss to steroidogenic failure, offering mechanistic clarity for Dhh-related infertility.

The functional divergence of Ptch receptors (Ptch1 and Ptch2) in Hh signaling has long intrigued researchers. Structurally, both receptors share conserved 12-transmembrane domains critical for cholesterol transport, yet diverge in their cytoplasmic C-terminal regions, which govern Smo inhibition efficiency [34, 35]. In mammals, Ptch1 broadly regulates Hh signaling during embryogenesis, while Ptch2 exhibits tissue-specific roles, such as primordial germ cell migration via its co-receptor Gas1 [25]. However, their functional overlap and receptor specificity in steroidogenic cells remain unresolved. Do Ptch1 and Ptch2 exhibit redundancy in Leydig cells, or do they mediate distinct signaling outcomes? Our study resolves this ambiguity. Despite both *ptch1* and *ptch2* were expressed in Leydig cells (Fig. 4A-B), functional assays revealed stark divergence: *ptch2* knockout abolished Dhh signaling responsiveness in TSL cells, whereas *ptch1* knockout had no effect (Fig. 4C-E). Genetic rescue experiments further confirmed this specificity—*dhh*$^{-/-}$;*ptch2*$^{-/-}$ testes exhibited fully restored morphology and steroidogenesis (Fig. 4F-R), demonstrating that Ptch2 alone compensates for Dhh loss. The exclusive reliance on Ptch2 may result from co-receptor interactions. For instance, a co-receptor, such as Boc, is essential for Ptch1 activity in murine primordial germ cell migration [25]. Nevertheless, further studies are required to elucidate the receptor specific to Dhh in the context of Leydig lineage commitment, utilizing Leydig cell-specific *ptch1/2* knockout models. It is noteworthy that *ptch1* mutant tilapias perished 6-8 days post-fertilization due to the absence of blood circulation [36]. Consequently, this study was unable to investigate the function of Ptch1 during testis development. Future research employing Leydig cell-specific *ptch1/2* knockout may clarify their interactions.

Gli is a nuclear transcription factor, characterized by the presence of a zinc finger domain located in the middle of the protein [37]. Downstream of the zinc finger domain is a phosphorylation cluster containing phosphorylation sites for protein kinase A and glycogen synthase kinase 3, which negatively regulate the transcriptional activity of Gli through phosphorylation [38]. In *Drosophila*, Ci is the sole Gli homolog, possessing both transcriptional activation and repression functions [39]. In vertebrates, there are three Gli homologs: Gli1, Gli2, and Gli3. Gli1 functions solely as a transcriptional activator because it lacks proteolytic processing domains. Gli2 has both activation and repression functions, while Gli3 primarily acts as a transcriptional repressor [40, 41]. However, there has been no research on the regulatory mechanism of Gli1/2/3 in SLCs differentiation. In this study, we found that although *gli1*, *gli2*, and *gli3* are all expressed

in Leydig cells (Figure 5A-C), the results from TSL cell lines with mutations in *gli1*, *gli2*, and *gli3* indicated that TSL-*gli1*$^{-/-}$, rather than TSL-*gli2*$^{-/-}$or TSL-*gli3*$^{-/-}$, failed to respond to Dhh signaling (Figure 5D). This suggests that Gli1 is the key transcription factor downstream of the Dhh signaling cascade in SLCs. These findings further elucidate the role of Gli1 as the key Dhh effector in teleost steroidogenesis and provide new insights into the plasticity of transcriptional regulation in vertebrates.

Sf1 and Dhh play important roles in Leydig cell commitment and testicular development [5, 10]. Studies suggest a potential interaction between these two factors. For example, in *Dhh*$^{-/-}$ XY mice, testicular development is impaired, with a significant reduction in the number of Leydig cells and a marked downregulation of *Sf1* expression [24]. In XX mouse ovaries where Smo is constitutively activated, a large number of ectopic Sf1-positive Leydig cells are generated [42]. Similarly, in *sf1*$^{-/-}$ XY tilapia, testicular development is impaired, with a significant reduction in Leydig cell numbers and down regulation of *dhh* expression [9]. These findings imply that Dhh and Sf1 may interact through feedback loops or co-regulatory mechanisms. However, direct evidence for the regulation of Sf1 by the Hh signaling pathway remains lacking. This study systematically elucidates the molecular mechanism by which the Dhh-Ptch2-Gli1 axis directly controls *sf1* expression. Transcriptomic profiling revealed a marked upregulation of *sf1* in Dhh-overexpressing TSL cells (Fig. S6), identifying it as a key downstream target of Hh signaling. Promoter analysis identified two conserved Gli-binding motifs (Fig. 5F) within the *sf1* promoter, and luciferase assays confirmed that Gli1 directly activates *sf1* transcription (Fig. 5G). Functional validation demonstrated that TSL-*sf1*$^{-/-}$ cells failed to differentiate even in WT testes, whereas TSL-OnSf1 cells restored Leydig cell differentiation and steroidogenesis in *dhh*$^{-/-}$ testes (Fig. 5H-J). These results establish Sf1 as both necessary and sufficient for Leydig cell differentiation.

Our findings highlight the importance of niche signals in regulating SLCs differentiation. The failure of TSL cells to differentiate in *dhh*$^{-/-}$ testes, unless activated by Dhh overexpression or SAG (Fig. 3), underscores the critical role of the local microenvironment in Leydig cell maturation. Interestingly, we observed that transplanted TSL cells could induce the local endogenous SLCs differentiation (Fig. 3), suggesting that TSL-derived signals may need a permissive niche for endogenous SLCs differentiation. This phenomenon deserves further investigation, as it may reveal novel paracrine factors essential for stem cell niche interactions.

MATERIALS AND METHODS

Animals

Nile tilapias (*Oreochromis niloticus*) were kept in recirculating freshwater systems at 26°C under a 12-h light/dark photoperiod. All animal experiments were conducted in accordance with the regulations of the Guide for Care and Use of Laboratory Animals prescribed by the Committee of Laboratory Animal Experimentation at Southwest University, China (IACUC-20181015-12).

Generation of mutant lines by CRISPR/Cas9 in Nile tilapia

The sequences of tilapia *dhh* (GenBank ID: 100707022) and *ptch2* (GenBank ID: 100692939) were retrieved from the NCBI. CRISPR/Cas9-mediated mutagenesis was performed as described previously [43]. Guide RNAs (gRNAs) targeting the first exon of *dhh* (GCGGGCCCGGTCCGCATCCC) and *ptch2* (GTCCCAGGGGCCGGCGTATT) were designed using ZiFit (http://zifit.partners.org/ZiFiT/). gRNA and Cas9 mRNA were synthesized following established protocols [43]. The primers listed in Table S1. A mixture of synthetic gRNA (500 ng/μl) and Cas9 mRNA (1000 ng/μl) was microinjected into one-cell-stage fertilized embryos. Mutants were validated by polyacrylamide gel electrophoresis (PAGE) and Sanger sequencing. F0 chimeric XY males were crossed with WT XX females to generate heterozygous F1 offspring. F1 siblings carrying a 13-bp deletion in *dhh* or a 25-bp deletion in *ptch2* were intercrossed to generate homozygous F2 mutants. For double mutants, $dhh^{+/-}$ XY males were mated with $ptch2^{+/-}$ XX females to obtain $dhh^{+/-}$;$ptch2^{+/-}$ offspring. These double heterozygotes were then intercrossed to generate $dhh^{-/-}$;$ptch2^{-/-}$ mutants.

Generation of mutant lines by pCas9-NtU6sgRNA system in TSL Cells

The tilapia stem Leydig cell line TSL was maintained in ESM4 medium as described [32]. Gene sequences for *ptch1* (GenBank ID: 100700194), *ptch2* (GenBank ID: 100692939), *gli1* (GenBank ID: 100710687), *gli2* (GenBank ID: 100704788), *gli3*

(GenBank ID: 100707331), and *sf1* (GenBank ID: 100534561) were retrieved from NCBI. Knockout plasmids targeting these genes were designed following established protocols [44]. gRNAs were generated using ZiFit, with the following exon-specific targets: *ptch1* (GGAGGCGCTCCTGCAGCACC, exon 3), *ptch2* (GTCCCAGGGGCCGGCGTATT, exon 1), *gli1* (TGACTCATGGATCAGGACCA, exon 2), *gli2* (GATTCGCCTGTCACCCCACG, exon 3), *gli3* (TGAGGAGCCCTCTACGTCTA, exon 2), and *sf1* (GGCTGTGTACTGGTACTGGG, exon 4; designed as previously described) [44]. Primers are listed in Table S1. Plasmids were transfected into TSL cells using the MDMP E-1 microchannel transfection instrument (MENDGENE) with transwell cell compartments (BIOFIT), per manufacturer guidelines. Post-transfection (48 hours), cells were selected in ESM4 medium containing 500 μg/mL G418 for 7 days. Single-cell clones were isolated via dilution and serial passage, followed by genomic DNA (gDNA) extraction and Sanger sequencing to confirm mutations.

Histological analyses of testes from WT, *dhh*$^{-/-}$, *ptch2*$^{-/-}$ and *dhh*$^{-/-}$;*ptch2*$^{-/-}$ XY fish

GSI was calculated for WT, *dhh*$^{-/-}$, *ptch2*$^{-/-}$ and *dhh*$^{-/-}$; *ptch2*$^{-/-}$ XY fish at 90 dah as: (gonad weight / body weight) × 100%. Testes were fixed in Bouin's solution for 24 hours at room temperature with agitation, dehydrated through an ethanol series, and embedded in paraffin. Sections (5 μm thickness) were stained with hematoxylin and eosin (H&E) and imaged using an Olympus BX53 microscope. Germ cell classification (spermatogonia, spermatocytes) followed established criteria [45].

Immunofluorescence

Testes from WT, *dhh*$^{-/-}$, WT+11-KT, *dhh*$^{-/-}$+11-KT, *ptch2*$^{-/-}$ and *dhh*$^{-/-}$; *ptch2*$^{-/-}$ XY fish at 90 dah were analyzed for germ cell marker Vasa, Leydig cell marker Cyp11c1, and meiosis marker Sycp3. Tissue fixation and embedding. Sections (5 μm) were deparaffinized, rehydrated, and subjected to antigen retrieval. After blocking with 5% bovine serum albumin (BSA; 30 minutes, room temperature), sections were incubated overnight at 4°C with rabbit polyclonal primary antibodies (Vasa, Cyp11c1, Sycp3;

1:1,000 dilution), validated previously [46]. Alexa Fluor 488-conjugated goat anti-rabbit secondary antibody (1:1,000; Invitrogen) was applied for 1 hour at 37°C, followed by DAPI nuclear counterstaining (1:1,000; Sigma-Aldrich). Fluorescence signals were imaged using an Olympus Fv3000 confocal microscope, and positive cells were quantified manually.

Fluorescence *in situ* hybridization (FISH) and IF

Testes from WT XY tilapia at 90 dah were fixed in 4% paraformaldehyde (Sigma) overnight at 4°C with agitation, paraffin-embedded, and sectioned (5 μm). FISH was performed as described [45]. Partial cDNA fragments of *ptch1*, *ptch2*, *gli1*, *gli2*, and *gli3* were cloned into the pGEM-T Easy vector. Sense (control) and antisense RNA probes were synthesized using a DIG RNA Labeling Kit (Roche) and T7 mMESSAGE mMACHINE Kit (Ambion). Signals were amplified with the TSA™ Plus TMR system (PerkinElmer) per manufacturer protocols (primers in Table S1). Concurrently, Leydig cell marker Cyp11c1 expression was assessed by IF.

11-KT and SAG rescue experiments

To rescue *dhh*$^{-/-}$ XY fish, offspring from *dhh*$^{+/-}$ XY male × *dhh*$^{+/-}$ XX female crosses were divided into two groups. The experimental group received 11-KT via immersion from 30 to 90 dah, with treatments refreshed every 2 days. 11-KT concentrations increased incrementally from 57 ng/L at 30 dah to 1254 ng/L by 90 dah (39.9 ng/L increase per treatment cycle; see Fig. 2, 5, S3). For SAG rescue, fish received intraperitoneal injections of 10 mg/kg SAG from 30 to 90 dah, with booster doses administered weekly. Testes were collected at 90 dah for morphological and histological evaluation.

TSL cell labeling, transplantation and IF

TSL, previously isolated from 3-month-old XY tilapia testes [32], was used to assess stem Leydig cell differentiation in WT and *dhh*$^{-/-}$ XY fish. TSL cells were treated as follows: (1) untreated TSL, (2) TSL + 0.5 μM SAG (Hh pathway agonist), (3) TSL-*On*Dhh (overexpressing tilapia Dhh), (4) TSL-*On*Sf1 (overexpressing tilapia Sf1), and

(5) TSL-*sf1*$^{-/-}$ (*sf1* mutation). Cells were labeled with PKH26 fluorescent dye (Sigma) and transplanted (5,000 cells per testis) into WT or *dhh*$^{-/-}$ XY tilapia via the urogenital tract [32]. For TSL-*On*Dhh, the Dhh ORF (1377 bp) was amplified from gDNA, cloned into pcDNA3.1 (Invitrogen), and transfected into TSL cells (primers in Table S1). At 10 days post-transplantation, testes were analyzed by IF to quantify Cyp11c1 positive cells among PKH26 positive populations.

GLI report assay

A firefly luciferase reporter plasmid (8×GLI) was generated by cloning eight tandem copies of the GLI-binding motif (GACCACCCA) into the pGL4.23 vector (minimal promoter). To validate 8×GLI functionality, TSL cells were transiently transfected with: (1) pGL4.23 (negative control), (2) 8×GLI, or (3) 8×GLI plus Dhh-overexpression plasmid (*On*Dhh), for 48 hours. The 8×GLI construct was further transfected into TSL (WT), TSL-*ptch1*$^{-/-}$, TSL-*ptch2*$^{-/-}$, TSL-*gli1*$^{-/-}$, TSL-*gli2*$^{-/-}$ or TSL-*gli3*$^{-/-}$, with or without *On*Dhh. Transfections included pRL-TK as an internal control. Luciferase activity was measured 48 hours post-transfection using the Dual Luciferase Assay System (Promega) and a Luminoskan™ Ascent luminometer (Thermo Fisher Scientific). Relative activity was calculated as firefly/Renilla luciferase ratios.

Western blot

The ORFs of Dhh (1377 bp) and Gli1 (4404 bp) were amplified from gDNA by PCR. Two tandem FLAG tag sequences (GATTATAAAGATGATGATAAA) were inserted flanking each ORF (after the start codon and before the stop codon) and cloned into the pcDNA3.1 vector (Invitrogen), generating pcDNA3.1-*On*Dhh and pcDNA3.1-*On*Gli1 (primers in Table S1). TSL cells were transiently transfected with pcDNA3.1-*On*Dhh or pcDNA3.1-*On*Gli1 for 48 hours. Protein expression was analyzed by Western blot following established methods [46]. Briefly, total protein lysates were separated by 15% SDS-PAGE, transferred to nitrocellulose membranes, and blocked with 5% BSA in TBST (10 mM Tris pH 7.9, 150 mM NaCl, 0.1% Tween-20) for 1 hour at 37°C. Membranes were incubated overnight at 4°C with rabbit anti-FLAG antibody (1:1000; Cell Signaling Technology), followed by HRP-conjugated goat anti-rabbit

secondary antibody (1:1000; Invitrogen) for 1 hour at 37°C. Signals were detected using the BeyoECL Plus Kit (Beyotime) and imaged on a Fusion FX7 system (Vilber Lourmat).

Measurement of 11-KT levels by ELISA

Blood was collected from the caudal vein of 90 dah XY fish (WT, *dhh*$^{-/-}$, *ptch2*$^{-/-}$, *dhh;ptch2*$^{-/-}$, WT+TSL, *dhh*$^{-/-}$+TSL, *dhh*$^{-/-}$+TSL+SAG, *dhh*$^{-/-}$+TSL-*On*Dhh and *dhh*$^{-/-}$+TSL-*sf1*$^{-/-}$), incubated at 4°C overnight, and centrifuged to isolate serum. Tissue fluid samples from WT and *dhh*$^{-/-}$ XY fish at 5, 10, 20, and 30 dah were similarly prepared. All samples were stored at −80°C until analysis. Serum and tissue fluid 11-KT levels were quantified using a 11-keto Testosterone ELISA Kit (Cayman) validated for teleost samples, per manufacturer instructions. Individual samples (serum or tissue fluid; n = 6 per genotype) were analyzed in triplicate on a single 96-well plate, with concentrations calculated from standard curves.

Transcriptome analyses

Tissue- and stage-specific expression of *dhh* was assessed using transcriptomic data from tilapia tissues (brain, heart, head kidney, kidney, liver, muscle, ovary, testis) and gonads at developmental stages spanning 5 to 360 dah [47, 48]. For global gene expression profiling, RNA was extracted from TSL-WT, TSL-*On*Dhh, TSL-*On*Gli1, and TSL + 0.5 μM SAG cells using RNAiso Plus (Takara). Libraries were sequenced on an Illumina platform (GENEBOOK Biotechnology), and clean reads were aligned to the reference genome with HISAT2. Gene expression levels (FPKM: fragments per kilobase per million mapped reads) were quantified using featureCounts. Differentially expressed genes (DEGs) were identified with edgeR (threshold: FDR < 0.05, |log2(foldchange)| ≥ 1.5).

Real-time PCR

Testes from WT and *dhh*$^{-/-}$ XY fish at 90 dah (n = 3 per genotype), along with TSL-WT, TSL-*On*Dhh, TSL-*On*Gli1, and TSL + 0.5 μM SAG cells, were analyzed for gene expression. Total RNA was extracted using RNAiso Plus (Takara), reverse-transcribed into cDNA (PrimeScript II 1st Strand cDNA Synthesis Kit; Takara), and amplified by real-time PCR on an ABI-7500 system (Applied Biosystems). Relative mRNA levels

were normalized to *β-actin* and calculated via the formula $R = 2^{-\Delta\Delta Ct}$ (primers in Table S1).

Dual luciferase report assay

The 5015-bp promoter region upstream of the *sf1* start codon was amplified and cloned into the pGL3-basic vector (Promega), generating pGL3-*sf1* (primers in Table S1). To assess Gli1 binding to the *sf1* promoter, HEK293 cells were co-transfected with pGL3-*sf1* and pcDNA3.1- *On*Gli1 using the TransIT-X2 transfection reagent (Mirus Bio). Control transfections included empty pcDNA3.1 and pGL3 vectors, with pRL-TK for normalization. Luciferase activity was measured 48 hours post-transfection.

Statistical analyses

Data are presented as mean ± SD from at least three independent replicates. Statistical significance was determined using unpaired two-tailed Student's *t*-tests in GraphPad Prism 5, with $P < 0.05$ and $P < 0.01$ indicating significant and highly significant differences, respectively.

Data availability statement

The data that support the findings of this study are available from the corresponding author upon reasonable request.

Acknowledgements

This research was funded by the National Key Research and Development Program of China (Grant No. 2022YFD1201600), the National Natural Science Foundation of China (Grant No. 32172969, 31972776, 32102780, 32473159).

Author contributions

Changle Zhao: Writing – original draft, Software, Resources, Methodology, Investigation, Formal analysis, Data curation. **Yongxun Chen**: Writing – original draft, Methodology, Data curation. **Lei Liu**: Data curation, Conceptualization. **Xiang Liu**: Software, Investigation. **Hesheng Xiao**: Software, Data curation. **Feilong Wang**: Investigation, Formal analysis. **Qin Huang**: Resources, Software. **Xiangyan Dai**: Resources, Investigation. **Wenjing Tao**: Resources, Funding acquisition. **Deshou Wang**: Supervision, Investigation, Funding acquisition. **Jing Wei**: Writing – review &

editing, Validation, Supervision, Project administration, Funding acquisition, Data curation, Conceptualization.

Conflict of interest

The authors declare no competing interest.

References

1. Inoue, M., Baba, T., and Morohashi, K.I. (2018). Recent progress in understanding the mechanisms of Leydig cell differentiation. Mol. Cell. Endocrinol *468*, 39-46.
2. Jiang, M.H., Cai, B., Tuo, Y., Wang, J., Zang, Z.J., Tu, X., Gao, Y., Su, Z., Li, W., Li, G., et al. (2014). Characterization of Nestin-positive stem Leydig cells as a potential source for the treatment of testicular Leydig cell dysfunction. Cell. Res *24*, 1466-1485.
3. Yao, S., Wei, X., Deng, W., Wang, B., Cai, J., Huang, Y., Lai, X., Qiu, Y., Wang, Y., Guan, Y., et al. (2022). Nestin-dependent mitochondria-ER contacts define stem Leydig cell differentiation to attenuate male reproductive ageing. Nat. Commun *13*, 4020.
4. Chen, P., Zirkin, B.R., and Chen, H. (2020). Stem Leydig Cells in the Adult Testis: Characterization, Regulation and Potential Applications. Endocr. Rev *41*, 22-32.
5. Parker, K.L., Rice, D.A., Lala, D.S., Ikeda, Y., Luo, X., Wong, M., Bakke, M., Zhao, L., Frigeri, C., Hanley, N.A., et al. (2002). Steroidogenic factor 1: an essential mediator of endocrine development. Recent. Prog. Horm. Res *57*, 19-36.
6. Houzelstein, D., Eozenou, C., Lagos, C.F., Elzaiat, M., Bignon-Topalovic, J., Gonzalez, I., Laville, V., Schlick, L., Wankanit, S., Madon, P., et al. (2024). A conserved NR5A1-responsive enhancer regulates SRY in testis-determination. Nat. Commun *15*, 2796.
7. Smith, O.E., Morin, F., Roussel, V., Bertucci, M.C., Boyer, A., and Murphy, B.D. (2023). The role of steroidogenic factor 1 (SF-1) in steroidogenic cell function of the testes and ovaries of mature mice. Reproduction *165*, 1-17.
8. Yu, Y., Lee, P.A., Huerta-Saenz, L., and Allen, N.G. (2023). A Novel Variant in NR5A1 Presenting as 46,XY Difference of Sex Development. JCEM. Case. Rep *1*, luad103.
9. Xie, Q.P., He, X., Sui, Y.N., Chen, L.L., Sun, L.N., and Wang, D.S. (2016). Haploinsufficiency of SF-1 Causes Female to Male Sex Reversal in Nile Tilapia, *Oreochromis niloticus*. Endocrinology *157*, 2500-2514.
10. Zhang, Y., and Beachy, P.A. (2023). Cellular and molecular mechanisms of Hedgehog signalling. Nat. Rev. Mol. Cell. Biol *24*, 668-687.
11. Briscoe, J., and Thérond, P.P. (2013). The mechanisms of Hedgehog signalling and its roles in development and disease. Nat. Rev. Mol. Cell. Biol *14*, 416-429.
12. Ingham, P.W., Nakano, Y., and Seger, C. (2011). Mechanisms and functions of Hedgehog signalling across the metazoa. Nat. Rev. Genet *12*, 393-406.
13. Finco, I., LaPensee, C.R., Krill, K.T., and Hammer, G.D. (2015). Hedgehog signaling and steroidogenesis. Annu. Rev. Physiol *77*, 105-129.

14. Carpenter, D., Stone, D.M., Brush, J., Ryan, A., Armanini, M., Frantz, G., Rosenthal, A., and de Sauvage, F.J. (1998). Characterization of two patched receptors for the vertebrate hedgehog protein family. Proc. Natl. Acad. Sci. USA *95*, 13630-13634.
15. Belgacem, Y.H., and Borodinsky, L.N. (2015). Inversion of Sonic hedgehog action on its canonical pathway by electrical activity. Proc. Natl. Acad. Sci. USA *112*, 4140-4145.
16. Cervantes, S., Lau, J., Cano, D.A., Borromeo-Austin, C., and Hebrok, M. (2010). Primary cilia regulate Gli/Hedgehog activation in pancreas. Proc. Natl. Acad. Sci. USA *107*, 10109-10114.
17. Umehara, F., Tate, G., Itoh, K., Yamaguchi, N., Douchi, T., Mitsuya, T., and Osame, M. (2000). A novel mutation of desert hedgehog in a patient with 46,XY partial gonadal dysgenesis accompanied by minifascicular neuropathy. Am. J. Hum. Genet *67*, 1302-1305.
18. Pachernegg, S., Georges, E., and Ayers, K. (2022). The Desert Hedgehog Signalling Pathway in Human Gonadal Development and Differences of Sex Development. Sex. Dev *16*, 98-111.
19. Mehta, P., Singh, P., Gupta, N.J., Sankhwar, S.N., Chakravarty, B., Thangaraj, K., and Rajender, S. (2021). Mutations in the desert hedgehog (DHH) gene in the disorders of sexual differentiation and male infertility. J. Assist. Reprod. Genet *38*, 1871-1878.
20. Pierucci-Alves, F., Clark, A.M., and Russell, L.D. (2001). A developmental study of the Desert hedgehog-null mouse testis. Biol. Reprod *65*, 1392-1402.
21. Wei, J., Wu, J., Ru, W., Chen, G., Gao, L., and Tang, D. (2022). Novel compound heterozygous mutations in the desert hedgehog (DHH) gene in cases of siblings with 46,XY disorders of sexual development. BMC. Med. Genomics *15*, 178.
22. Cong, G., Zhu, X., Chen, X.R., Chen, H., and Chong, W. (2025). Mechanisms and therapeutic potential of the hedgehog signaling pathway in cancer. Cell. Death. Discov *11*, 40.
23. Nieuwenhuis, E., Motoyama, J., Barnfield, P.C., Yoshikawa, Y., Zhang, X., Mo, R., Crackower, M.A., and Hui, C.C. (2006). Mice with a targeted mutation of patched2 are viable but develop alopecia and epidermal hyperplasia. Mol. Cell. Biol *26*, 6609-6622.
24. Yao, H.H., Whoriskey, W., and Capel, B. (2002). Desert Hedgehog/Patched 1 signaling specifies fetal Leydig cell fate in testis organogenesis. Genes. Dev *16*, 1433-1440.
25. Kim, Y., Lee, J., Seppala, M., Cobourne, M.T., and Kim, S.H. (2020). Ptch2/Gas1 and Ptch1/Boc differentially regulate Hedgehog signalling in murine primordial germ cell migration. Nat. Commun *11*, 1994.
26. Ruiz i Altaba, A., Sánchez, P., and Dahmane, N. (2002). Gli and hedgehog in cancer: tumours, embryos and stem cells. Nat. Rev. Cancer *2*, 361-372.
27. Hui, C.C., and Angers, S. (2011). Gli proteins in development and disease. Annu. Rev. Cell. Dev. Biol *27*, 513-537.
28. Barsoum, I., and Yao, H.H. (2011). Redundant and differential roles of transcription factors Gli1 and Gli2 in the development of mouse fetal Leydig cells. Biol. Reprod *84*, 894-899.
29. Gennotte, V., François, E., Rougeot, C., Ponthier, J., Deleuze, S., and Mélard, C.

(2012). Sperm quality analysis in XX, XY and YY males of the Nile tilapia (Oreochromis niloticus). Theriogenology *78*, 210-217.
30. Li, M., Sun, L., Zhou, L., and Wang, D. (2024). Tilapia, a good model for studying reproductive endocrinology. Gen. Comp. Endocrinol *345*, 114395.
31. Sun, Y.L., Jiang, D.N., Zeng, S., Hu, C.J., Ye, K., Yang, C., Yang, S.J., Li, M.H., and Wang, D.S. (2014). Screening and characterization of sex-linked DNA markers and marker-assisted selection in the Nile tilapia (*Oreochromis niloticus*). Aquaculture *433*, 19-27.
32. Huang, Q., Yang, Z., Wang, J., Luo, Y., Zhao, C., Li, M., Xiao, H., Tao, W., Wang, D., and Wei, J. (2020). Establishment of a stem Leydig cell line capable of 11-ketotestosterone production. Reprod. Fertil. Dev *32*, 1271-1281.
33. Zheng, Q., Xiao, H., Shi, H., Wang, T., Sun, L., Tao, W., Kocher, T.D., Li, M., and Wang, D. (2020). Loss of Cyp11c1 causes delayed spermatogenesis due to the absence of 11-ketotestosterone. J. Endocrinol *244*, 487-499.
34. Qi, X., Schmiege, P., Coutavas, E., and Li, X. (2018). Two Patched molecules engage distinct sites on Hedgehog yielding a signaling-competent complex. Science *362*.
35. Fleet, A.J., and Hamel, P.A. (2018). The protein-specific activities of the transmembrane modules of Ptch1 and Ptch2 are determined by their adjacent protein domains. J. Biol. Chem *293*, 16583-16595.
36. Liu, X., Zhao, C., Liu, L., Peng, X., Li, J., Tao, W., Wang, D., and Wei, J. (2024). Nile Tilapia (*Oreochromis niloticus*) Patched1 Mutations Disrupt Cardiovascular Development and Vascular Integrity through Smoothened Signaling. Int. J. Mol. Sci *25*.
37. Kinzler, K.W., Ruppert, J.M., Bigner, S.H., and Vogelstein, B. (1988). The GLI gene is a member of the Kruppel family of zinc finger proteins. Nature *332*, 371-374.
38. Niewiadomski, P., Kong, J.H., Ahrends, R., Ma, Y., Humke, E.W., Khan, S., Teruel, M.N., Novitch, B.G., and Rohatgi, R. (2014). Gli protein activity is controlled by multisite phosphorylation in vertebrate Hedgehog signaling. Cell. Rep *6*, 168-181.
39. Huangfu, D., and Anderson, K.V. (2006). Signaling from Smo to Ci/Gli: conservation and divergence of Hedgehog pathways from *Drosophila* to vertebrates. Development *133*, 3-14.
40. Niewiadomski, P., Niedziółka, S.M., Markiewicz, Ł., Uśpieński, T., Baran, B., and Chojnowska, K. (2019). Gli Proteins: Regulation in Development and Cancer. Cells *8*.
41. Pan, Y., and Wang, B. (2007). A novel protein-processing domain in Gli2 and Gli3 differentially blocks complete protein degradation by the proteasome. J. Biol. Chem *282*, 10846-10852.
42. Barsoum, I.B., Bingham, N.C., Parker, K.L., Jorgensen, J.S., and Yao, H.H. (2009). Activation of the Hedgehog pathway in the mouse fetal ovary leads to ectopic appearance of fetal Leydig cells and female pseudohermaphroditism. Dev. Biol *329*, 96-103.
43. Li, M., Yang, H., Zhao, J., Fang, L., Shi, H., Li, M., Sun, Y., Zhang, X., Jiang, D., Zhou, L., et al. (2014). Efficient and heritable gene targeting in tilapia by CRISPR/Cas9. Genetics *197*, 591-599.
44. Zhang, Z., Wang, J., Li, J., Liu, X., Liu, L., Zhao, C., Tao, W., Wang, D., and Wei, J.

(2023). Establishment of an Integrated CRISPR/Cas9 Plasmid System for Simple and Efficient Genome Editing in Medaka In Vitro and In Vivo. Biology *12*.
45. Zhao, C., Liu, X., Liu, L., Li, J., Liu, X., Tao, W., Wang, D., and Wei, J. (2023). Smoothened mediates medaka spermatogonia proliferation via Gli1-Rgcc-Cdk1 axis. Biol. Reprod *109*, 772-784.
46. Dai, S., Qi, S., Wei, X., Liu, X., Li, Y., Zhou, X., Xiao, H., Lu, B., Wang, D., and Li, M. (2021). Germline sexual fate is determined by the antagonistic action of dmrt1 and foxl3/foxl2 in tilapia. Development *148*.
47. Tao, W., Yuan, J., Zhou, L., Sun, L., Sun, Y., Yang, S., Li, M., Zeng, S., Huang, B., and Wang, D. (2013). Characterization of gonadal transcriptomes from Nile tilapia (*Oreochromis niloticus*) reveals differentially expressed genes. PloS. One *8*, e63604.
48. Tao, W., Chen, J., Tan, D., Yang, J., Sun, L., Wei, J., Conte, M.A., Kocher, T.D., and Wang, D. (2018). Transcriptome display during tilapia sex determination and differentiation as revealed by RNA-Seq analysis. BMC. Genomics *19*, 363.

Figure legends

Fig. 1. Mutation of *dhh* resulted in testicular developmental disorders.

(A-B) Morphological analysis of the testes from WT ($dhh^{+/+}$) and $dhh^{-/-}$ XY fish at 90 dah.

(C-D') Histological examination of gonadal sections from WT and $dhh^{-/-}$ XY fish at 90 dah using H&E staining. Sg, spermatogonia; Sc, spermatocyte.

(E-J') Expression of germ cell marker Vasa (E-F'), Leydig cell marker Cyp11c1 (G-H') and meiosis cell marker Sycp3 (I-J') in testes sections from WT and $dhh^{-/-}$ XY fish at 90 dah by immunofluorescence.

(K) Gonadosomatic index (GSI) of the testes from WT and $dhh^{-/-}$ XY fish at 90 dah (n=5 fish/genotype).

(L-N) Statistical analysis of the Vasa (E-F'), Cyp11c1 (G-H') and Sycp3 (I-J') positive cells (n=5 fish/genotype).

(O) Serum 11-KT level of WT and $dhh^{-/-}$ XY fish at 90 dah (n=6 fish/genotype). Values were presented as mean ± SD. Differences were determined by two-tailed independent Student's t-test. **, $P < 0.01$. Scale bars, (A-B), 1 cm; (C-J), 50 μm.

Fig. 2. 11-KT partially rescued differentiation of germ cells, but not Leydig cells. Treat the WT and $dhh^{-/-}$ XY fish from 30 dah to 90 dah by immersion with DMSO or equal volume of 11-KT, which simulates the normal concentration in WT XY tilapia, changing the water every two days, and then perform morphological and histological experiments on their testes.

(A-C') Histological examination of gonadal sections from WT +11-KT, *dhh*$^{-/-}$ and *dhh*$^{-/-}$ +11-KT XY fish at 90 dah using H&E staining. Sg, spermatogonia; Sc, spermatocyte. Scale bars, 50 μm.

(D-L') Expression of Vasa (D-F'), Cyp11c1 (G-I') and Sycp3 (J-L') in testes sections from WT +11-KT, *dhh*$^{-/-}$ and *dhh*$^{-/-}$ +11-KT XY fish at 90 dah by immunofluorescence. Scale bars, 50 μm.

(M) GSI of the testes from WT +11-KT, *dhh*$^{-/-}$ and *dhh*$^{-/-}$ +11-KT XY fish at 90 dah (n=3 fish/genotype).

(N-P) Statistical analysis of the Vasa (D-F'), Cyp11c1 (G-I') and Sycp3 (J-L') positive cells (n=3 fish/genotype).

Values were presented as mean ± SD. Different letters above the error bar indicate statistical differences at $P < 0.05$ as determined by one-way ANOVA followed by Tukey test.

Fig. 3. Mutation of *dhh* resulted in the failure of SLCs differentiation.

The normal Leydig stem cells (TSL), TSL with 0.5 μM SAG (TSL+SAG) and TSL overexpressing tilapia Dhh (TSL-*On*Dhh) were labeled with PKH26 and selectively transplanted into the 90 dah WT and *dhh*$^{-/-}$ XY fish testes, followed by immunofluorescence experiments conducted 10 days post-transplantation.

(A) Flowchart of the experiment.

(B1-E3) Expression of Cyp11c1 and PKH26 in testes sections from WT +TSL, *dhh*$^{-/-}$ +TSL, *dhh*$^{-/-}$+TSL+SAG, *dhh*$^{-/-}$+TSL-Dhh-OE and WT +TSL-*sf1*$^{-/-}$ XY fish at 90 dah by immunofluorescence. Scale bars, 10 μm.

(F) The percentage of Cyp11c1 positive (Cyp11c1^{+}) cells among PKH26 positive (PKH26^{+}) cells in B1-E3 (n=5 fish/genotype).

(G) Serum 11-KT level in B1-E3 (n=5 fish/genotype).

(H-I) Treat the WT and *dhh*$^{-/-}$ XY fish from 30 dah to 90 dah by intraperitoneal injection with 10mg/kg SAG or an equal volume of DMSO, with a supplementary injection every 7 days, and then perform morphological and histological experiments on their testes. (H) Expression of Cyp11c1 in testes sections from *dhh*$^{-/-}$+SAG XY fish at 90 dah by immunofluorescence. Scale bars, 50 μm. (I) Statistical analysis of the Cyp11c1 positive cells (n=5 fish/genotype).

Values were presented as mean ± SD. Different letters above the error bar indicate statistical differences at $P < 0.05$ as determined by one-way ANOVA followed by Tukey test.

Fig. 4. Ptch2 is the specific receptor for Dhh in SLCs.

(A-B) Co-staining of Leydig cell marker Cyp11c1 and *ptch1* and *ptch2* on the 90 dah (adult) testes by immunofluorescence (IF) and RNA fluorescence in situ hybridization (FISH), respectively. The cells outlined by dashed lines in the figure are typical Leydig cells. Scale bars, 4 μm.

(C) Schematic diagram of D and E.

(D) TSL cells were transiently transfected with pGL4.23 (a plasmid lacking Gli binding site, as a negative control), a Gli-responsive luciferase reporter (8xGLI) or 8xGLI and *On*Dhh (overexpression of tilapia Dhh) for 48 h, respectively. Relative luciferase levels were measured at 48 h post transfection. Values were presented as mean ± SD (n=3). Differences were determined by two-tailed independent Student's t-test. **, $P < 0.01$.

(E) The TSL-WT, TSL-*ptch1*$^{-/-}$ and TSL-*ptch2*$^{-/-}$ cells were transiently transfected with 8xGLI or 8xGLI and *On*Dhh for 48 h, respectively. Relative luciferase levels were measured at 48 h posttransfection. Values were presented as mean ± SD (n=4). Differences were determined by two-tailed independent Student's t-test. NS, no significant difference; *, $P < 0.05$; **, $P < 0.01$.

(F-G') Histological examination of gonadal sections from *ptch2*$^{-/-}$ and *dhh*$^{-/-}$;*ptch2*$^{-/-}$ XY fish at 90 dah using H&E staining. Sg, spermatogonia; Sc, spermatocyte. Scale bars, 50 μm.

(H-M') Expression of Vasa (I-K'), Cyp11c1 (L-N') and Sycp3 (O-Q') in testes sections from *ptch2*$^{-/-}$ and *dhh*$^{-/-}$;*ptch2*$^{-/-}$ XY fish at 90 dah by immunofluorescence. Scale bars, 50 μm.

(N) GSI of the testes from WT, *ptch2*$^{-/-}$ and *dhh*$^{-/-}$, *ptch2*$^{-/-}$ XY fish at 90 dah (*n*=4 fish/genotype).

(O-Q) Statistical analysis of the Vasa (H-I'), Cyp11c1 (J-K') and Sycp3 (L-M') positive cells (*n*=6 fish/genotype).

(R) Serum 11-KT level in WT, *ptch2*$^{-/-}$ and *dhh*$^{-/-}$, *ptch2*$^{-/-}$ XY fish at 90 dah (*n*=6 fish/genotype).

Values were presented as mean ± SD. Differences were determined by two-tailed independent Student's t-test. NS, no significant difference.

Fig. 5. Gli1 is the specific transcription factor for Dhh and its regulation of Sf1 in SLCs.

(A-C) Co-staining of Cyp11c1 and *gli1, gli2* and *gli3* on the 90 dah testes by IF and FISH, respectively. The cells outlined by dashed lines in the figure are typical Leydig cells. Scale bars, 4 μm.

(D) The TSL-WT, TSL-*gli1*$^{-/-}$, TSL-*gli2*$^{-/-}$ and TSL-*gli3*$^{-/-}$ cells were transiently transfected with 8xGLI or 8xGLI and *On*Dhh for 48 h, respectively. Relative luciferase levels were measured at 48 h posttransfection. Values were presented as mean ± SD (n=4). Differences were determined by two-tailed independent Student's t-test. NS, no significant difference; **, $P < 0.01$.

(E) Volcanic plot of differentially expressed genes (DEGs) in TSL-*On*Dhh, TSL-*On*Gli1 and TSL+ SAG compared to TSL-WT.

(F) Schematic illustration of the *sf1* promoter. B1 and B2 were the predicted Gli1 binding sites.

(G) Effects of Gli1 on the transcriptional activity of tilapia *sf1* promoter in HEK293 cells. Values were presented as mean ± SD (n=4). **, $P < 0.01$.

TSL with *sf1* mutation (TSL-*sf1*$^{-/-}$) and TSL overexpressing tilapia Sf1 (TSL-*On*Sf1) were labeled with PKH26 and selectively transplanted into the 90 dah WT and *dhh*$^{-/-}$ XY fish testes, followed by immunofluorescence experiments conducted 10 days post-transplantation.

(H-I) Expression of Cyp11c1 and PKH26 in testes sections from WT +TSL-*sf1*$^{-/-}$ and *dhh*$^{-/-}$+TSL-*On*Sf1 XY fish at 90 dah by immunofluorescence. Scale bars, 10 μm.

(J) The percentage of Cyp11c1^{+} cells among PKH26^{+} cells in K-L (*n*=5 fish/genotype).

Fig. S1. Sequence analysis and mRNA expression profile of Nile tilapia *dhh*.

(A) Dhh amino acid sequence alignment. Amino acids are numbered in the right margin. Deletions are indicated by dashes, shaded areas indicate shared sequences. The amino-terminal hedge domain is underlined by dotted line, with the signal peptide region in the front and the autocatalytic carboxy-terminal domain (hog) in the back. The box indicates the autocatalytic site of an absolutely conserved Gly-Cys-Phe tripeptide. At the end of the alignment are percentage identity values of the full-length and hedge domain of tilapia Dhh to the orthologue from other species.

(B) Phylogenetic analysis of Dhh. The phylogenetic tree was constructed using the neighbor-joining method within the MEGA7.0 program. Node values represent percent bootstrap confidence derived from 1000 replicates.

(C-D) The RPKM (reads per kb per million reads) values of tilapia *dhh* in various

adult tissues (C) and XY and XX gonads at 5, 7, 20, 30, 90, 180, 300 dah (days after hatching) (D) in transcriptome sequencing data which were sequenced using Illumina 2000 HiSeq technology in our previous study (Tao et al., 2013).

Fig. S2. Establishment of the Nile tilapia *dhh* mutant line by CRISPR/Cas9 system.

(A) Schematic representation of gRNA targeting the Nile tilapia *dhh* locus. The gRNA was designed to target exon 1. The translation start codon ATG and stop codon TAA were indicated by arrows. The PAM (protospacer adjacent motif) site was marked by green box. DNA sequence alignment of the three mutant lines with WT. The added sequences were marked by red letter, and the deleted sequences were indicated in red dotted lines. One had a 4-bp addition, one had an 8-bp deletion, and the other had a 13-bp deletion.

(B) Schematic diagram showing the breeding plans of *dhh* F0 to F2 fish.

(C) Homozygous mutants of F2 fish were screened by PAGE. The first lane is DNA marker, the second lane is $dhh^{+/+}$ fish, the third lane is $dhh^{+/-}$ fish, and the fourth lane is $dhh^{-/-}$ fish.

(D) Sanger sequencing results of *dhh* genes from WT and the 13-bp deletion homozygous mutant fishes.

(E) The *dhh* ORF sequence in WT was indicated in black and the frameshift-altered sequence for the 13-bp deletion *dhh* ORF was indicated in red.

(F) The relative mRNA expression of *dhh* in WT and the 13-bp deletion homozygous mutant fishes by RT-qPCR. Values were presented as mean ± SD (n=3). **, $P < 0.01$.

Fig. S3. The expression levels of Cyp11c1 in the testis and the levels of 11-KT in tissue fluid from WT XY fish at 5, 10, 20, and 30 dah.

(A-C) Expression of Leydig cell marker Cyp11c1 in testes sections from WT XY fish at 5, 10 and 20 dah by immunofluorescence. Scale bars, 50 μm.

(D) Tissue fluid 11-KT level from $dhh^{+/+}$ and $dhh^{-/-}$ XY fish at 5, 10, 20 and 30 dah (n=6 fish/genotype). Values were presented as mean ± SD. Differences were determined by two-tailed independent Student's t-test. NS, no significant difference.

Fig. S4. RT-PCR analyses of Hh pathway genes in TSL cells. *β-actin* served as a loading control, and RNAs from TSL cells were used as templates for negative controls. The numbers in parentheses indicate the PCR cycles.

Fig. S5. Establishment of the TSL *ptch1*, *ptch2*, *gli1*, *gli2*, *gli3* and *sf1* mutant lines.

(A-F) Schematic representation of gRNAs targeting the *ptch1*, *ptch2*, *gli1*, *gli2*, *gli3*

and *sf1* locus. The gRNAs were designed to target ORF (open reading frame). The PAM (protospacer adjacent motif) sites were marked by red letter. Sanger sequencing of *ptch1*, *ptch2*, *gli1*, *gli2*, *gli3* and *sf1* single mutant alleles in single cell clones. PCR amplicons from DNA templates of the six cell clones were directly used for sequencing.

Fig. S6. Establishment of the Nile tilapia *ptch2* mutant line by CRISPR/Cas9 system.

(A) Schematic representation of gRNA targeting the Nile tilapia *ptch2* locus. The gRNA was designed to target exon 1. The translation start codon ATG and stop codon TGA were indicated by arrows. The PAM site was marked by green box. DNA sequence alignment of the five mutant lines with WT. The added sequences were marked by red letter, and the deleted sequences were indicated in red dotted lines.

(B) Schematic diagram showing the breeding plans of *ptch2* F0 to F2 fish.

(C) DNA sequencing showed the 25-bp deletion within the *ptch2* ORF in the homozygous mutant compared to the WT.

(D) Schematic of the prediction of the intact Ptch2 protein in the WT and the truncated Ptch2 protein in the homozygous mutants.

(E) Homozygous mutants of F2 fish were screened by PAGE. The first lane is DNA marker, the second lane is $ptch2^{+/+}$ fish, the third lane is $ptch2^{+/-}$ fish, and the fourth lane is $ptch2^{-/-}$ fish. "*" indicates heteroduplex, and arrows indicate homoduplex.

Fig. S7. (A-A') Histological examination of gonadal sections from WT XY fish at 90 dah using H&E staining. Sg, spermatogonia; Sc, spermatocyte. (B-D') Expression of Vasa (B-B'), Cyp11c1 (C-C') and Sycp3 (D-D') in testes sections from WT XY fish at 90 dah by immunofluorescence. Scale bars, 50 μm.

Fig. S8. Transcriptome data analyses and verification by RT-qPCR.

(A) Hierarchical clustering of gene expression in the TSL-WT, TSL-*On*Dhh, TSL-*On*Gli1 and TSL+ 0.5 μM SAG. Blue indicates decreased expression, and red indicates increased expression.

(B) Cluster heatmap of the upregulated DEGs in Fig. 5E.

(C) qRT-PCR validation. Values were presented as mean ± SD (n = 3).

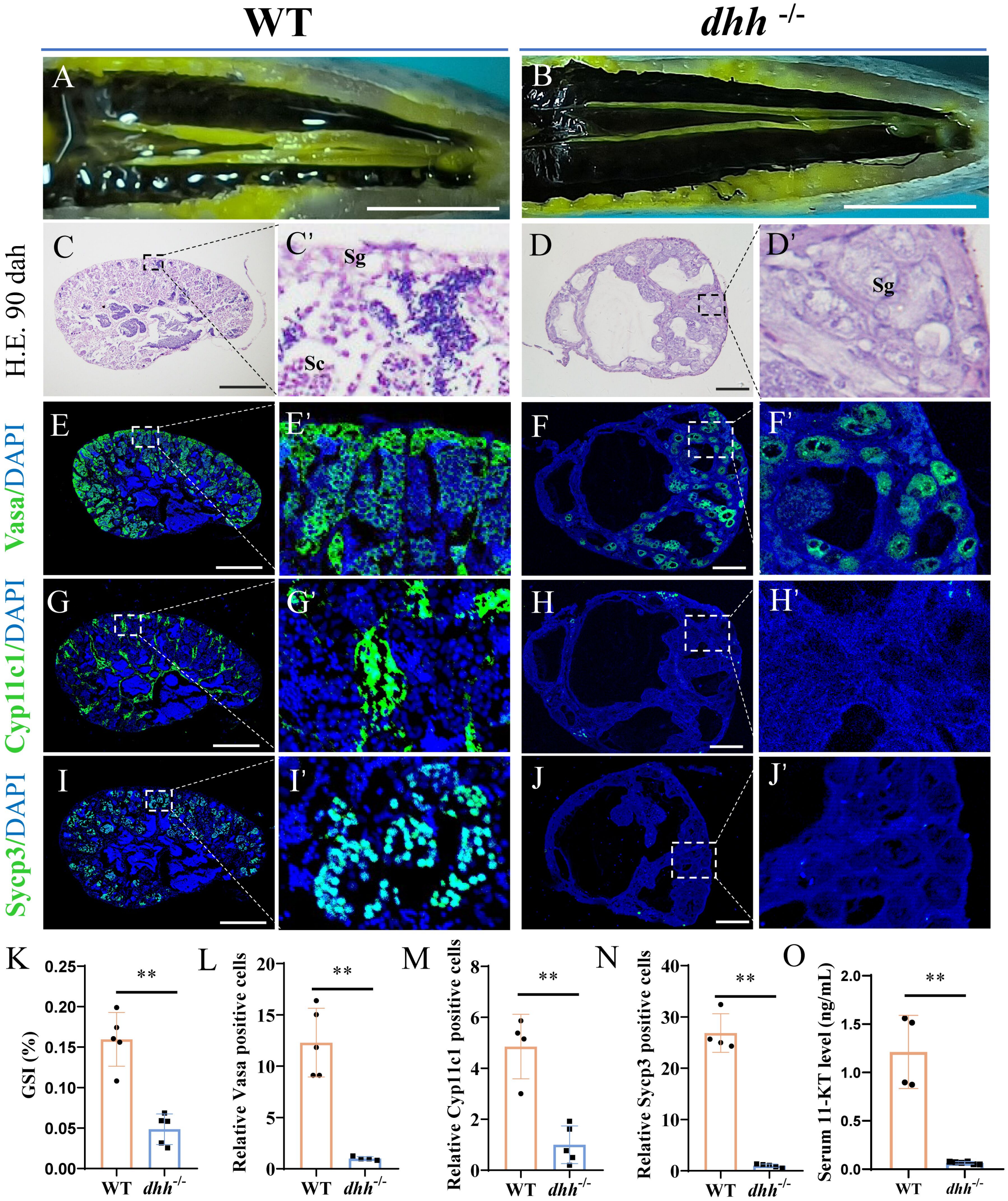
WT
dhh -/-
A
B
H.E. 90 dah
C
C'
Sg
Sc
D
D'
Sg
Vasa/DAPI
E
E'
F
F'
Cyp11c1/DAPI
G
G'
H
H'
Sycp3/DAPI
I
I'
J
J'
K
GSI (%)
0.25
0.20
0.15
0.10
0.05
0.00
**
WT
dhh-/-
L
Relative Vasa positive cells
20
15
10
5
0
**
WT
dhh-/-
M
Relative Cyp11c1 positive cells
8
6
4
2
0
**
WT
dhh-/-
N
Relative Sycp3 positive cells
40
30
20
10
0
**
WT
dhh-/-
O
Serum 11-KT level (ng/mL)
2.0
1.5
1.0
0.5
0.0
**
WT
dhh-/-

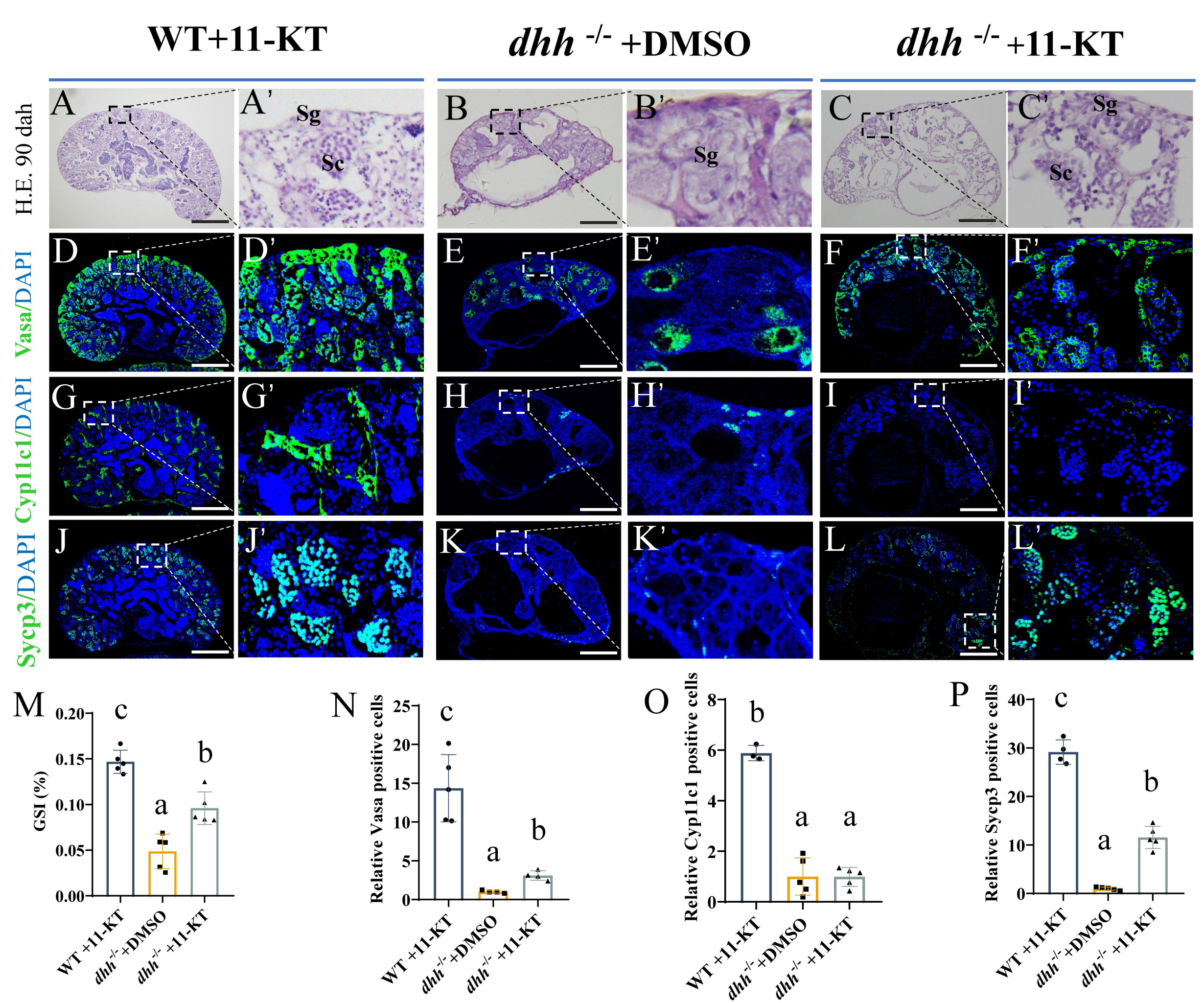
WT+11-KT
dhh -/- +DMSO
dhh -/- +11-KT
H.E. 90 dah
Vasa/DAPI
Cyp11c1/DAPI
Sycp3/DAPI
A
A'
Sg
Sc
B
B'
Sg
C
C'
Sg
Sc
D
D'
E
E'
F
F'
G
G'
H
H'
I
I'
J
J'
K
K'
L
L'
M
GSI (%)
0.20
0.15
0.10
0.05
0.00
c
a
b
WT +11-KT
dhh-/- +DMSO
dhh-/- +11-KT
N
Relative Vasa positive cells
25
20
15
10
5
0
c
a
b
WT +11-KT
dhh-/- +DMSO
dhh-/- +11-KT
O
Relative Cyp11c1 positive cells
8
6
4
2
0
b
a
a
WT +11-KT
dhh-/- +DMSO
dhh-/- +11-KT
P
Relative Sycp3 positive cells
40
30
20
10
0
c
a
b
WT +11-KT
dhh-/- +DMSO
dhh-/- +11-KT

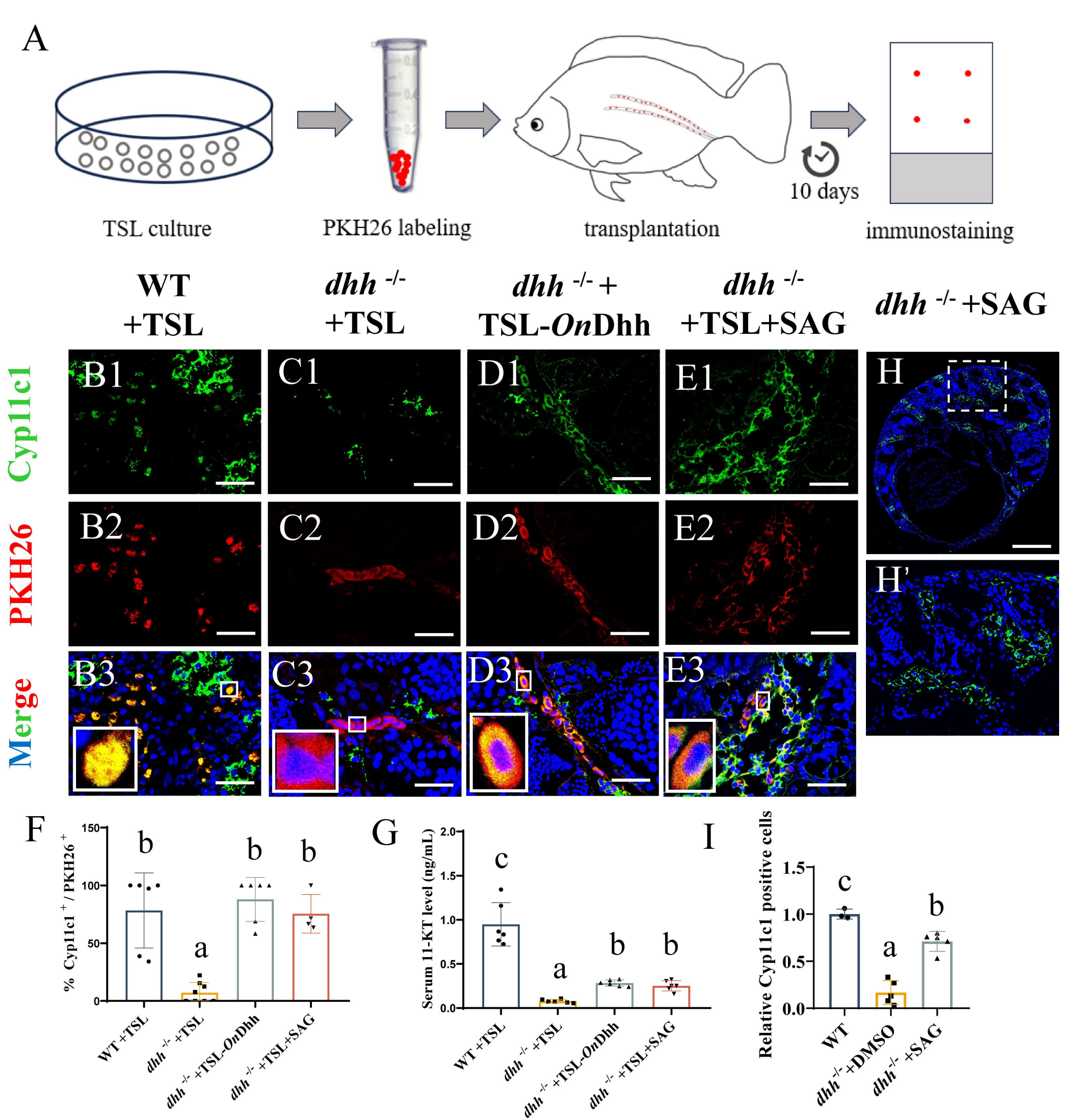
A
TSL culture
PKH26 labeling
transplantation
10 days
immunostaining
WT +TSL
dhh -/- +TSL
dhh -/- + TSL-OnDhh
dhh -/- +TSL+SAG
dhh -/- +SAG
Cyp11c1
PKH26
Merge
B1
C1
D1
E1
H
B2
C2
D2
E2
H'
B3
C3
D3
E3
F
% Cyp11c1 + / PKH26 +
150
100
50
0
b
a
b
b
WT +TSL
dhh -/- +TSL
dhh -/- +TSL-OnDhh
dhh -/- +TSL+SAG
G
Serum 11-KT level (ng/mL)
2.0
1.5
1.0
0.5
0.0
c
a
b
b
WT +TSL
dhh -/- +TSL
dhh -/- +TSL-OnDhh
dhh -/- +TSL+SAG
I
Relative Cyp11c1 positive cells
1.5
1.0
0.5
0.0
c
a
b
WT
dhh -/- +DMSO
dhh -/- +SAG

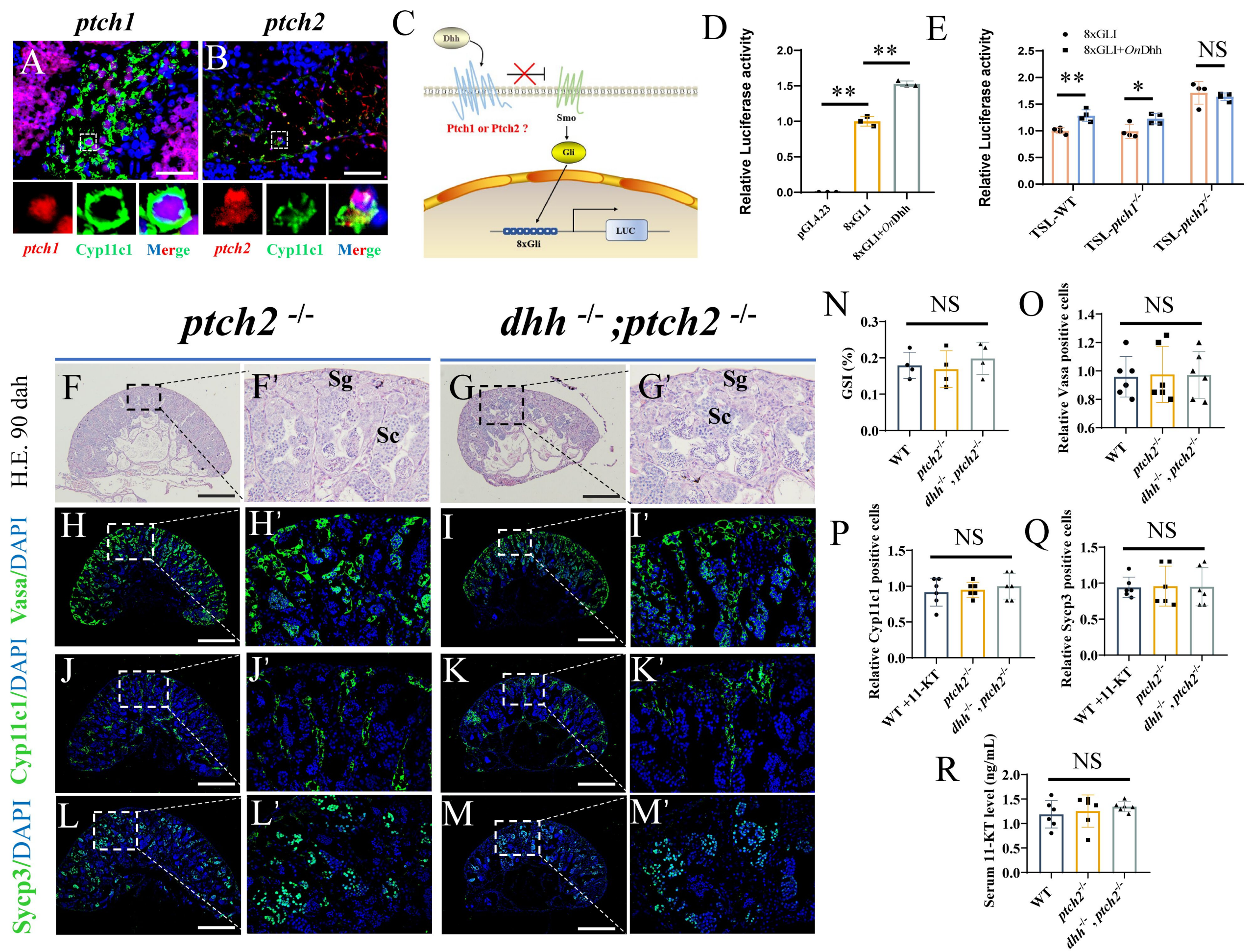
ptch1
ptch2
A
B
ptch1
Cyp11c1
Merge
ptch2
Cyp11c1
Merge
C
Dhh
Ptch1 or Ptch2 ?
Smo
Gli
8xGli
LUC
D
Relative Luciferase activity
pGL4.23
8xGLI
8xGLI+OnDhh
E
8xGLI
8xGLI+OnDhh
NS
Relative Luciferase activity
TSL-WT
TSL-ptch1-/-
TSL-ptch2-/-
ptch2 -/-
dhh -/- ;ptch2 -/-
H.E. 90 dah
Vasa/DAPI
Cyp11c1/DAPI
Sycp3/DAPI
Sg
Sc
N
NS
GSI (%)
WT
ptch2-/-
dhh-/- ,ptch2-/-
O
NS
Relative Vasa positive cells
P
NS
Relative Cyp11c1 positive cells
WT +11-KT
Q
NS
Relative Sycp3 positive cells
R
NS
Serum 11-KT level (ng/mL)

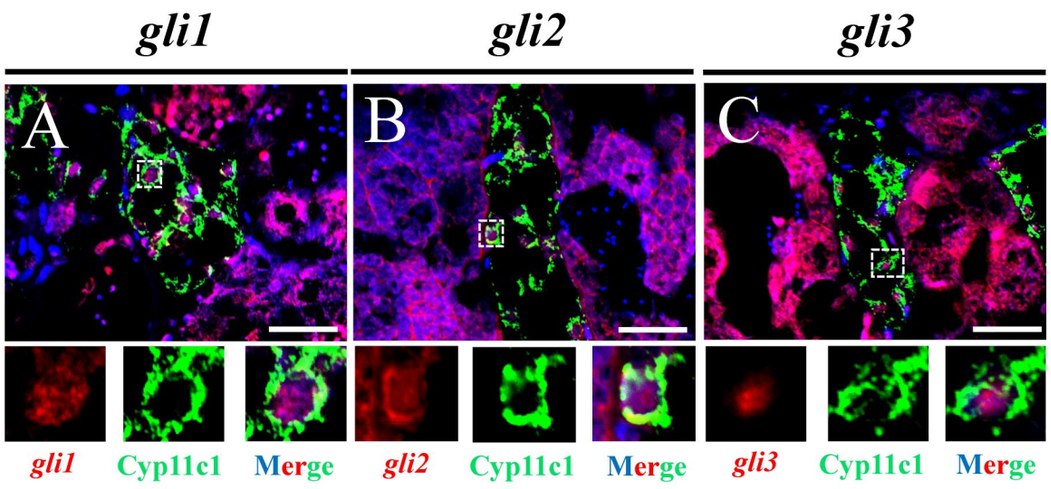

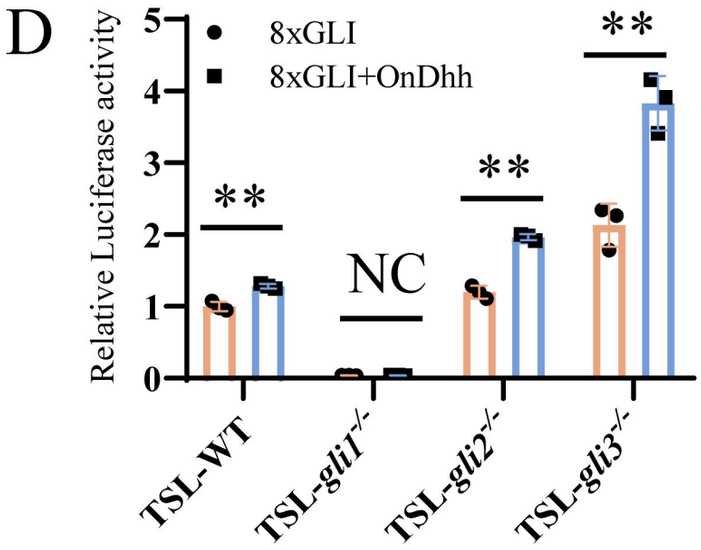

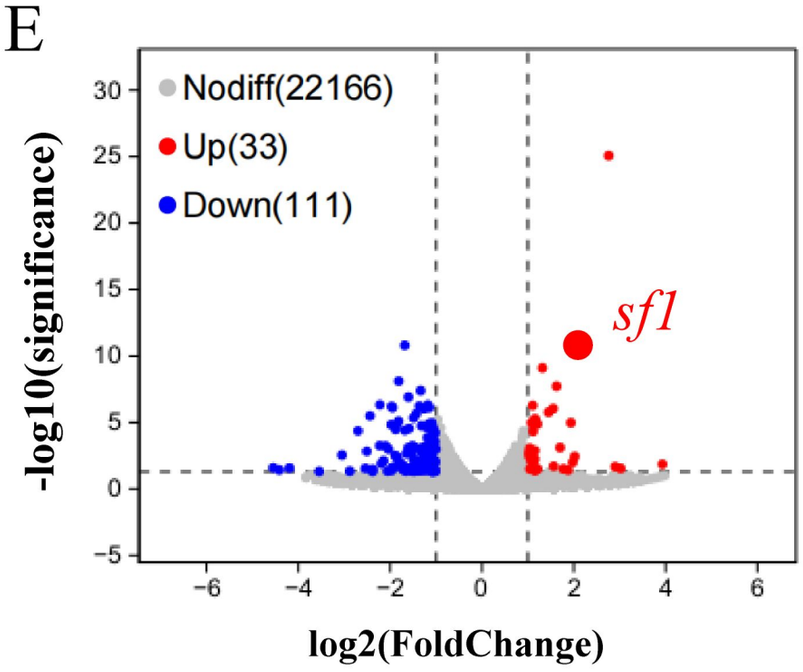
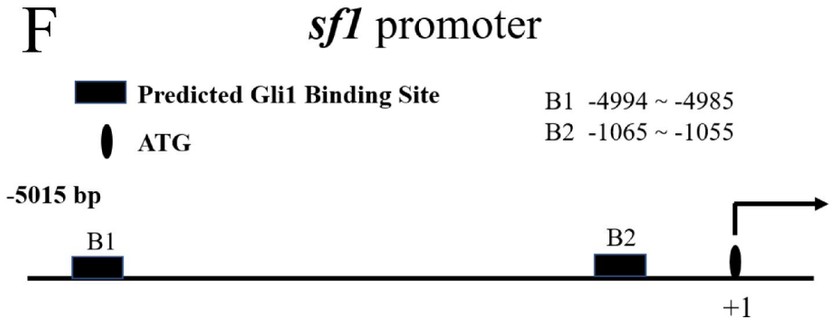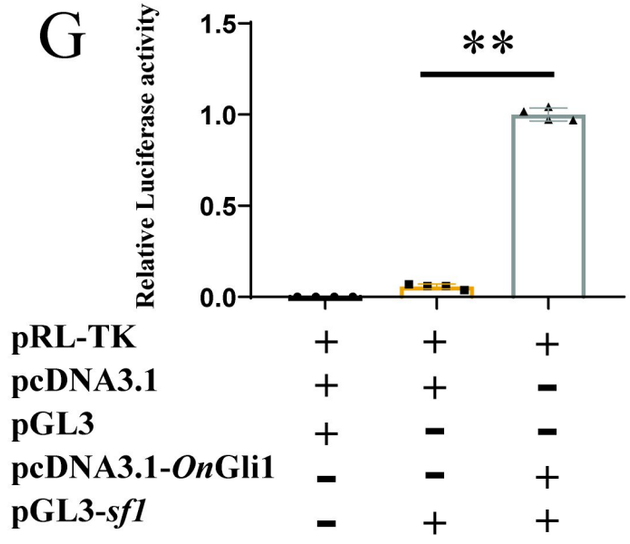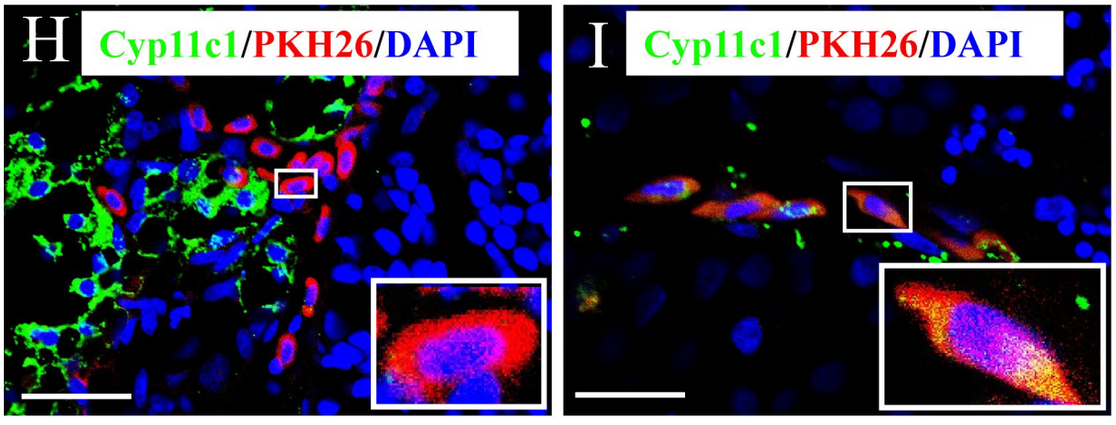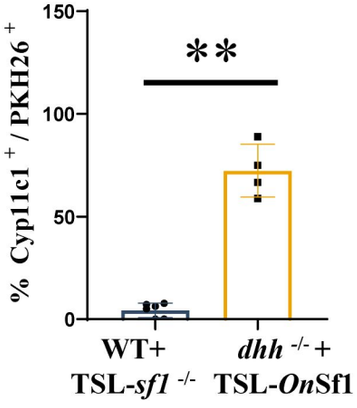
TSL-*On*Dhh
and TSL-*On*Gli1
and TSL+SAG
VS. TSL-WT